Available online at www.sciencedirect.com

SciVerse ScienceDirect

Journal of the European Ceramic Society 32 (2012) 2505–2512

www.elsevier.com/locate/jeurceramsoc

Mechanical and microwave dielectric properties of SiCf/SiC composites with BN interphase prepared by dip-coating process

Haitao Liu [a,b,*], Hao Tian [a]

[a] *Key Laboratory of Advanced Ceramic Fiber and Composites, College of Aerospace and Materials Engineering, National University of Defense Technology, Changsha 410073, China*

[b] *Science and Technology on Scramjet Laboratory, College of Aerospace and Materials Engineering, National University of Defense Technology, Changsha 410073, China*

Received 4 January 2012; received in revised form 6 February 2012; accepted 10 February 2012
Available online 7 March 2012

Abstract

The BN interphase of SiC fiber-reinforced SiC matrix (SiCf/SiC) composites was fabricated by dip-coating process with boric acid and urea as precursor. The results show that the tensile strength of SiC fiber decreases about 30% after BN coating treatment, but the BN coating has little influence on the electrical resistivity of SiC fiber. Compared with the as-received SiCf/SiC composites, the SiCf/SiC composites with BN interphase exhibit a toughened fracture behavior, and the flexural strength is about 2 times that of the as-received SiCf/SiC composites. From the microstructural analysis, it can be confirmed that the BN interphase plays a key part in weakening interfacial bonding, which can improve the mechanical properties of SiCf/SiC composites remarkably. Owing to the close dielectric properties between SiC and BN, the complex permittivity of SiCf/SiC composites with and without the BN interphase is similar.

Keywords: A. Precursors-organic; B. Composites; C. Mechanical properties; C. Dielectric properties; D. SiC; E. Functional applications

1. Introduction

SiC has excellent mechanical strength at elevated temperature, high oxidation resistance, high corrosion resistance, high thermal conductivity, low thermal expansion and high thermal shock resistance.[1,2] In addition, due to the excellent semiconductivity and relatively stable dielectric properties at elevated temperature, SiC also has many practical and potential applications for microwave absorption at high temperature.[3–14] However, owing to the inherent brittle failure behavior of monolithic SiC ceramic, it has been gradually substituted by SiCf/SiC composites, which can significantly improve the toughness of monolithic SiC ceramic.[15–17]

For SiCf/SiC composites, the interphase between the fiber and matrix is one of the key factors that determine the material properties. The appropriate interphase allows for crack deflection, fiber pullout and fiber–matrix debonding, which can provide excellent mechanical properties for SiCf/SiC composites[17]; at the same time, as one of important constituents in composites, the interphase also affects the dielectric properties of SiCf/SiC composites remarkably.

Pyrocarbon (PyC) and BN with layered crystal structures are the most commonly used and effective interphase materials for SiCf/SiC composites.[17] However, PyC interphase is not appropriate to being used in SiCf/SiC composites for microwave absorbing applications, because the continuous PyC interphase with high electrical conductivity can lead to strong microwave reflection of SiCf/SiC composites.[18] Consequently, BN with low dielectric constant characteristics is the ideal interphase material of SiCf/SiC composites for microwave absorbing applications.

Chemical vapor deposition (CVD) is the primary process to prepare BN interphase for SiCf/SiC composites.[19–22] However, there are still some disadvantages, such as the CVD process may require some hazardous precursor, and the reactants or gaseous products may affect the substrate materials at deposition temperature. In addition, it is difficult to control the pressure and flow rates of the reactants to attain good infiltration into yarns to form uniform coating on the individual fiber.[23]

* Corresponding author. Tel.: +86 731 84576440.
E-mail address: xzddlht@163.com (H. Liu).

0955-2219/$ – see front matter © 2012 Elsevier Ltd. All rights reserved.
doi:10.1016/j.jeurceramsoc.2012.02.009

Table 1
Properties of KD-2 SiC fiber.

Type	KD-2
Diameter (μm)	14–16
Number of filaments (fil/yarn)	∼1200
Tensile strength (MPa)	1500–1900
Density (g/cm^3)	∼2.55
C/Si atom	∼1.23
Chemical compositions of fiber surface layer	Silicon-based oxide
Processing temperature	∼1400 °C

In this study, BN interphase of SiCf/SiC composites was prepared by dip-coating process in boric acid and urea solutions followed by nitridation at nitrogen atmosphere. The effects of dip-coating process on the morphology and chemical compositions of fiber coating, tensile strength of SiC fiber and mechanical properties of SiCf/SiC composites were investigated. In addition, the electrical resistivity of SiC fiber with BN coating and complex permittivity of SiCf/SiC composites with BN interphase were studied, to the best our knowledge, which are rarely reported before.

2. Experimental

The reinforcements used to prepare 2D-SiCf/SiC composites were plain-weave KD-2 SiC fiber cloths, and the properties of KD-2 SiC fiber (from National University of Defense Technology, China) are shown in Table 1. Polycarbosilane (PCS), the precursor of SiC matrix, with relative molecular mass ∼1300 and softening point ∼210 °C, was synthesized in our laboratory. The 2D-SiCf/SiC composites were fabricated by precursor infiltration and pyrolysis (PIP) process, and the detailed process could be found in Ref. 24. The fiber volume fraction and porosity in the SiCf/SiC composites are about 45% and 18%, respectively.

Prior to PIP, the BN coating was deposited on the SiC fiber by dip-coating process. Boric acid (H_3BO_3, Tian Jin Hengxing Chemical preparation Co., LTD, China) and urea ($CO(NH_2)_2$, BASF Chemical Corp., Germany) were employed as the boron and nitrogen sources of BN, respectively. Boric acid and urea (3:1, wt ratio) were dissolved in the mixture of ethanol and deioned water (2:1, vol. ratio), and the concentration of solution is 0.8 mol/L.

The degreased SiC fiber plain-weave fabrics were dipped in the precursor solution of BN and ultrasonically vibrated for 15 min. Then the sample was drawn from the solution with a constant speed of 30 cm/min by a low speed motor and dried in air for 12 h. Finally, the coated fabrics were placed in a furnace for nitridation at different temperature at a rate of 5 °C/min under nitrogen atmosphere.

Scanning electron microscopy (SEM) work was done using a HITACHI FEG S4800 SEM. The chemical compositions of coating were analyzed by EDS equipped with SEM. An investigation of bonding in the nitridation production from BN precursor was performed via Fourier transform infrared (FT-IR) spectroscopy (Nicolet Avatar-360 FT-IR). The phases of

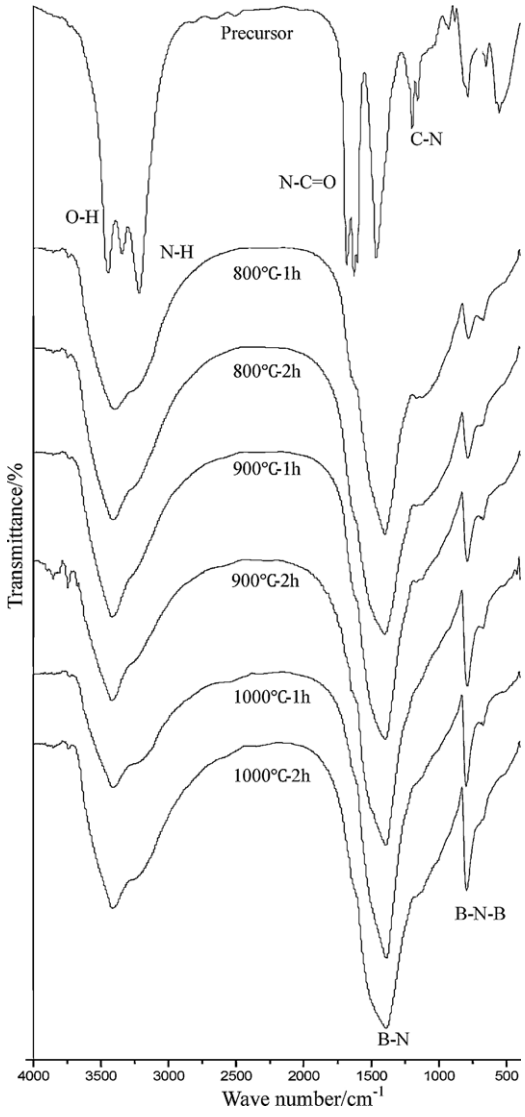

Fig. 1. The FT-IR spectra of production from boric acid and urea at different nitridation temperature and time.

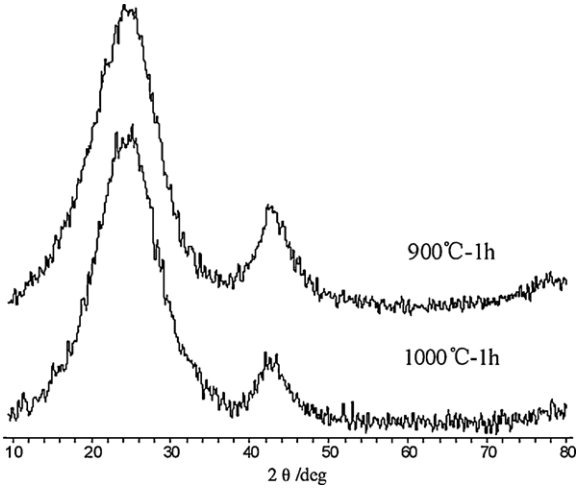

Fig. 2. The XRD patterns of production from boric acid and urea at nitridation temperature of 900 °C and 1000 °C.

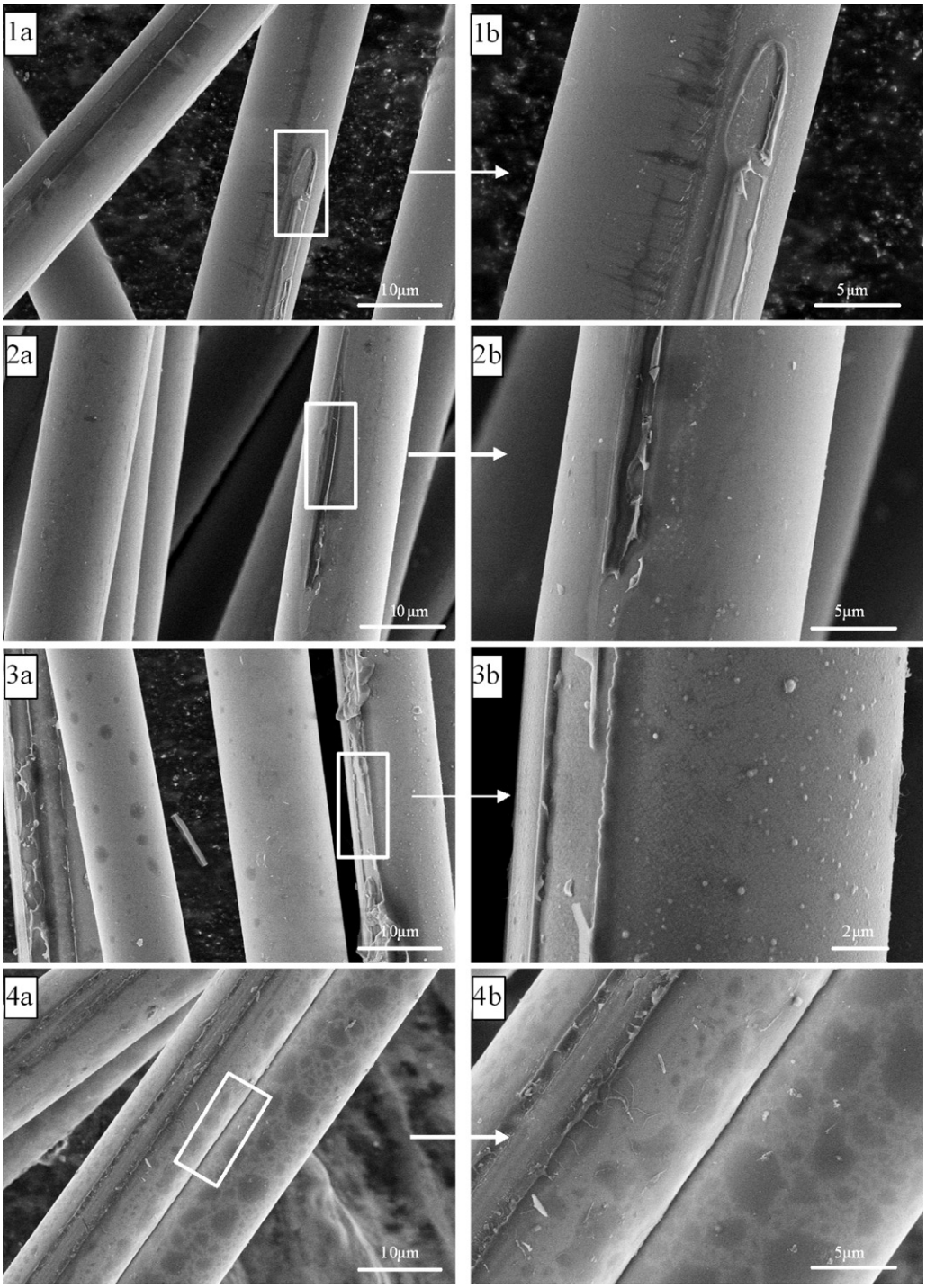

Fig. 3. SEM micrographs of the BN coating with different dipping-annealing times.

the nitridation production from BN precursor were characterized by X-ray diffraction (XRD) analysis using monochromatic Cu Kα radiation with a D8 ADVANCE diffractometer. X-ray photoelectron spectroscopy (XPS) analysis was done using a VG ESCA-LAB MK II apparatus with Al Kα radiation and calibrated against Au $4f_{7/2}$ and Cu $2p_{3/2}$ lines. Raman spectra were recorded with a Raman spectrometer HR 800 (Jobin-Yvon company, France) in backscattering geometry at 532 nm excitation wavelength. The laser beam was focused in air at normal incidence on a small area of the fiber surface (ca. 1 μm^2), and the laser beam power was 10 mW. The specimens for transmission electron microscope (TEM) observations followed the preparation procedure described by Dietrich et al.[25] TEM imaging was performed using a JEOL JEM-2010 high-resolution microscope operating at 200 kV.

Tensile strength of fiber was performed at room temperature with a MTS-Adamel DY-22 machine (Ivry sur Seine, France) equipped with a 5 N load cell. The crosshead speed

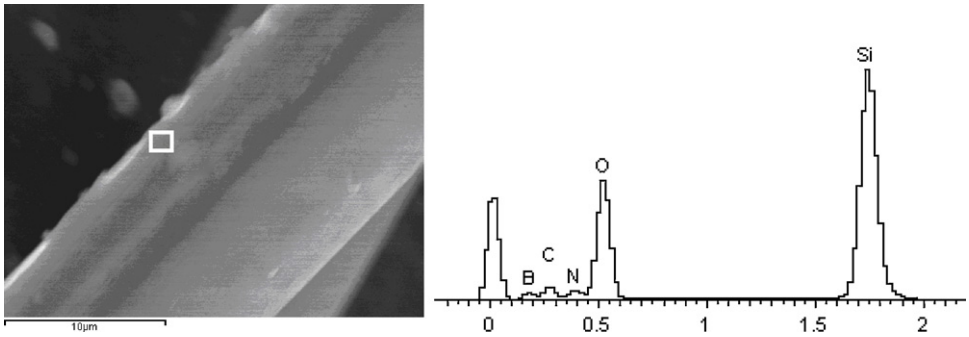

Fig. 4. EDS analysis of BN coating.

was 0.5 mm/min. In each case, 20–25 samples were tested with a 20 mm gauge length. The electrical resistivity measurement of SiC fiber followed the method described by Chollon et al.[10] Three-point bending of SiCf/SiC composites was carried out at ambient temperature. The sample geometry was about 60^{l} mm × 4^{w} mm × 3^{t} mm. The support span was 50 mm, and the crosshead speed was 0.5 mm/min. The complex permittivity of SiCf/SiC composites was measured at frequency between 8.2 and 18 GHz using the waveguide method with a HP8720ET network analyzer.

3. Results and discussion

3.1. Effects of nitridation temperature and time on the BN formation from boric acid and urea

The FT-IR spectra of production from boric acid and urea at different nitridation temperature and time are shown in Fig. 1. It can be found that the absorption peaks around 780 and 1380 cm^{-1} are detected when nitridation temperature is above 800 °C, which are assigned to the B–N bonds of t-BN according to Ref. 23. The integrated area under B–N absorption peak increases with increasing nitridation temperature, which indicates that the yield of BN increases with the increase of nitridation temperature, but the increasing tendency is not obvious when nitridation temperature is above 900 °C. In Fig. 1, no peaks corresponding to cubic BN near 1356 cm^{-1} are observed.

The XRD patterns of production from boric acid and urea at nitridation temperature of 900 °C and 1000 °C are shown in Fig. 2. There are no obvious differences between the two patterns. Two broad bands around 2θ values of 26° and 42° are detected, which correspond to the (0 0 2) and (1 1 0) reflections of t-BN, respectively.[23] The broad bands show that the crystallization of BN is not complete.

From the results of FT-IR and XRD analysis, the nitridation condition of 1000 °C for 1 h is chosen to prepare the BN coating for SiC fiber.

3.2. Characteristics of the BN coating

3.2.1. SEM and EDS analysis

Effects of dipping-annealing times on the morphology of BN coating are shown in Fig. 3. After one time of dipping-annealing treatment, one layer of smooth and thin coating can be found, but the coating is not continuous (Fig. 3a and b). After two times of dipping-annealing treatment, the continuous and uniform coating is formed, but elongated surface defects can be detected on some filaments (Fig. 3c and d). After three times of dipping-annealing treatment, the coating about 0.4 μm in thickness is formed on the surface of SiC fiber, but spalling and delamination phenomena can be detected (Fig. 3e and f). After four times of dipping-annealing treatment, the fiber bridging is observed (Fig. 3g and h). From the SEM analysis above, it can be concluded that the extent of stripping or cracking of the coating increases with increasing dipping-annealing times, which should be ascribed to the greater volume contraction from the evaporation transformation of organic in the thicker coating and the higher thermal stress associated with the incompatibility in the coefficients of thermal expansion between the coating and fiber. EDS analysis of the coating with three times of dip-coating treatment is shown in Fig. 4, and B and N are detected.

3.2.2. XPS analysis

Survey XPS spectra recorded from the surface of SiC fiber after three times of dip-coating treatment are shown in Fig. 5a. Photoelectron peaks from B 1s, N 1s, C 1s and O 1s are clearly recognized in the spectra. The intense B 1s component at 190.2 eV (Fig. 5b) corresponds to an atomic circle surrounding the boron atom consisting of only nitrogen atoms, similar to that occurring in h-BN.[26] The N 1s peak can be fitted into two sub peaks at 399.0 and 399.8 eV (Fig. 5c), which should be assigned to the N–B and N–H bonds, respectively.[27] The N–H bonds may be attributed to the incomplete decomposition of urea. The presence of the weak C 1s and O 1s peaks indicates that a small quantity of carbon and oxygen impurity is distributed in the coating.

3.2.3. Raman analysis

Raman spectra of SiC fiber after three times of dip-coating treatment are shown in Fig. 6. A strong peak at about 1370 cm^{-1} is detected, corresponding to in-plane B–N stretching vibration in h-BN (E_{2g2} modes).[20] In addition, a weak peak detected at around 3440 cm^{-1} should be assigned to N–H bonds, which is in agreement with the results of XPS analysis.

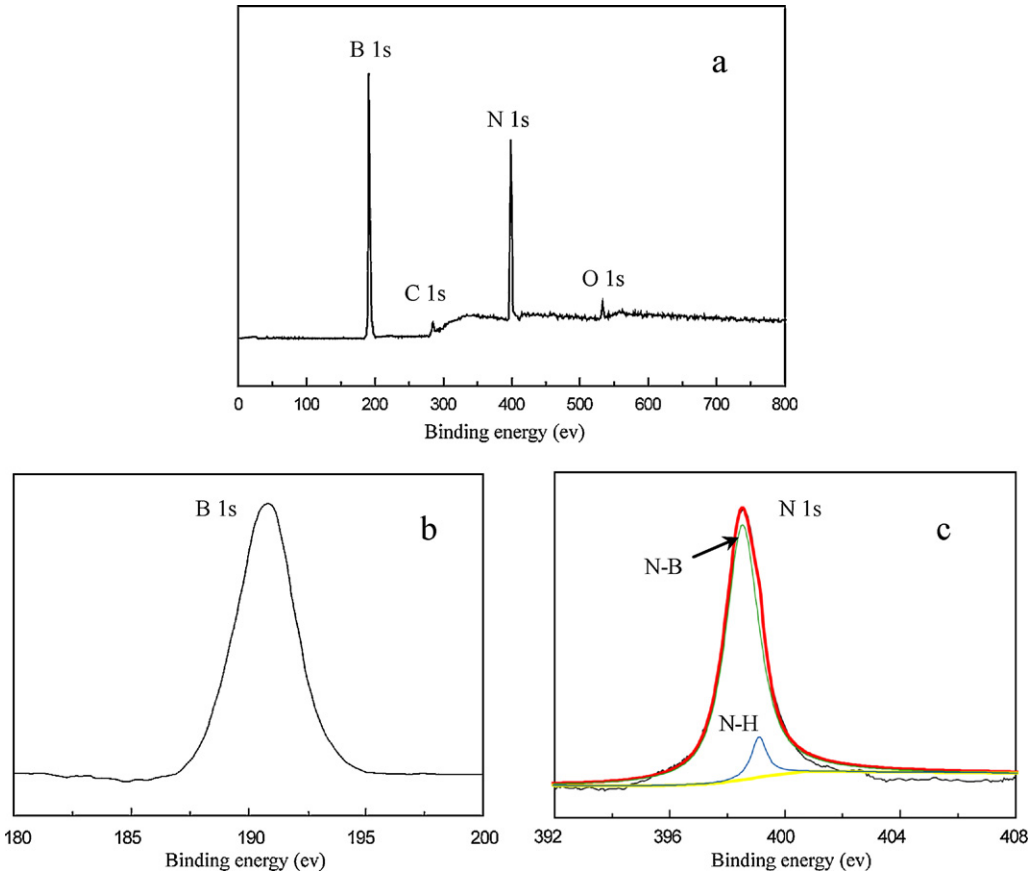

Fig. 5. XPS spectra of BN coating.

3.2.4. TEM analysis

TEM cross-sectional images of the SiC fiber after three times of dip-coating treatment are shown in Fig. 7. The coating about 400 nm in thickness adheres especially well to the fiber surface (Fig. 7a), which is agreement with the SEM observations of fiber coating. High-resolution images of the coating (Fig. 7b) reveal that t-BN exists in the coating, but the crystallization is not complete. The TEM observations of the coating are agreement with the FT-IR and XRD analysis of the nitridation production from boric acid and urea.

According to the analysis results above, the BN coating with turbostratic and amorphous hybrid structure deposited on the SiC fiber can be confirmed.

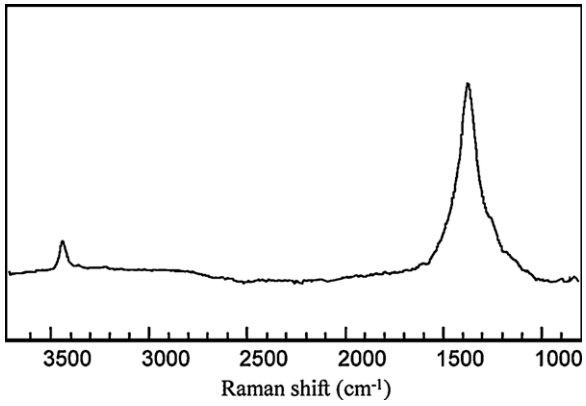

Fig. 6. Raman spectra of BN coating.

3.3. Effects of dipping-annealing times on the mechanical and electrical properties of SiC fiber

In Fig. 8, the relative tensile strength of the coated SiC fiber is shown as a function of dipping-annealing times. It can be found that the relative tensile strength decreases with the increase of dipping-annealing times, and the decreasing speed slows down gradually. The relative tensile strength is about 70% and 60% after one time and four times of dipping-annealing treatment, respectively. The degradation of tensile strength may probably be ascribed to the thermal stress damage from the volume contraction of coating and chemical damage from the formation process of BN.

The effects of dipping-annealing times on the electrical resistivity of SiC fiber are shown in Fig. 9. It can be found that there are no obvious differences of the electrical resistivity between SiC fiber without and with BN coating, which are ascribed to the similar electrical properties between SiC and BN.[28]

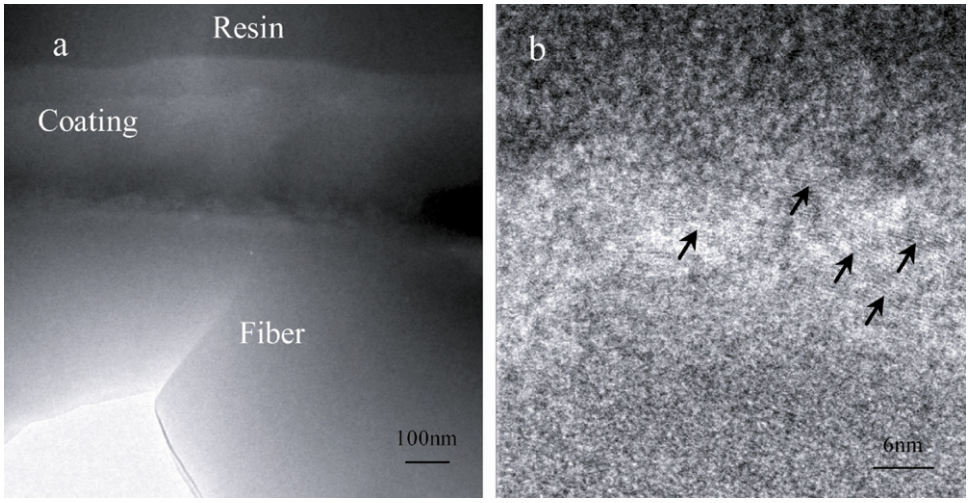

Fig. 7. TEM cross-sectional images of the coated SiC fiber.

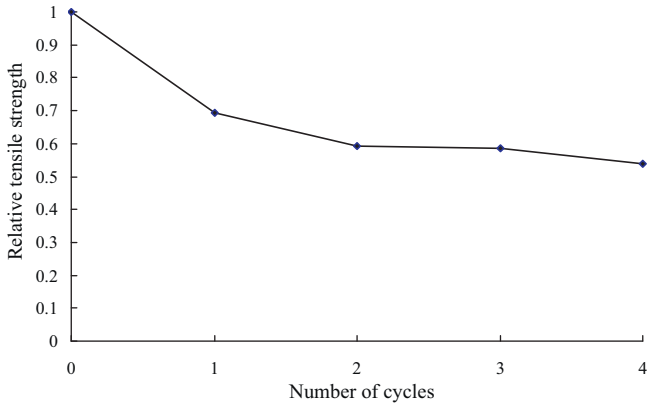

Fig. 8. Effects of dipping-annealing times on the tensile strength of SiC fiber.

3.4. Effects of BN interphase on the mechanical properties of SiCf/SiC composites

The flexural strength of SiCf/SiC composites with BN interphase prepared by different dipping-annealing times is shown in Fig. 10. It can be found that the flexural strength increases firstly and then decreases with the increase of dipping-annealing times of BN interphase. The maximum of flexural strength can be attained when three times of BN interphase treatment are performed, which is about 2 times that of SiCf/SiC composites without BN interphase.

The fracture surface morphology of the SiCf/SiC composites without and with BN interphase is shown in Fig. 11. For the as-received SiCf/SiC composites, the fracture surface is very even, and nearly no pullout fiber can be found (Fig. 11a). As shown in Fig. 11b, a strong interfacial bonding occurs at the interface, and no interfacial debonding behavior can be observed. Contrarily, concerning the SiCf/SiC composites with BN interphase, the fracture surface shows an evident fiber pullout (Fig. 11c), and the maximal length of the pullout fiber can exceed 10 μm. The interfacial debonding phenomena are obvious between the fiber and matrix (Fig. 11d).

In general, the mechanical properties of the continuous fiber reinforced ceramic matrix composites are determined by the in situ fiber strength and interfacial characteristics. In our previous work,[24] it has been concluded that the stronger interfacial bonding and low in situ fiber strength occur in the SiCf/SiC composites without appropriate interphase, which make the fiber

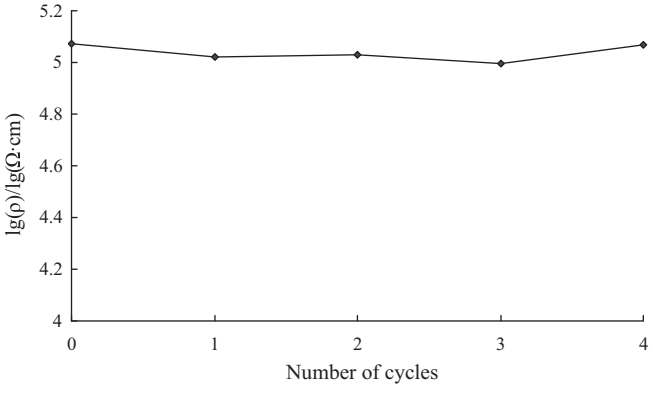

Fig. 9. Effects of dipping-annealing times on the electrical resistivity of SiC fiber.

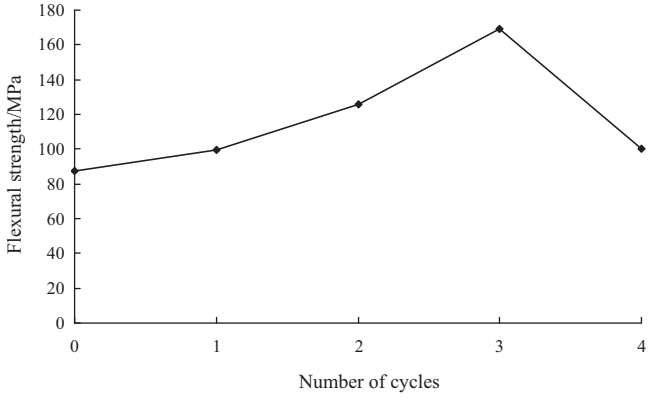

Fig. 10. Flexural strength of SiCf/SiC composites with BN interphase prepared by different dipping-annealing times.

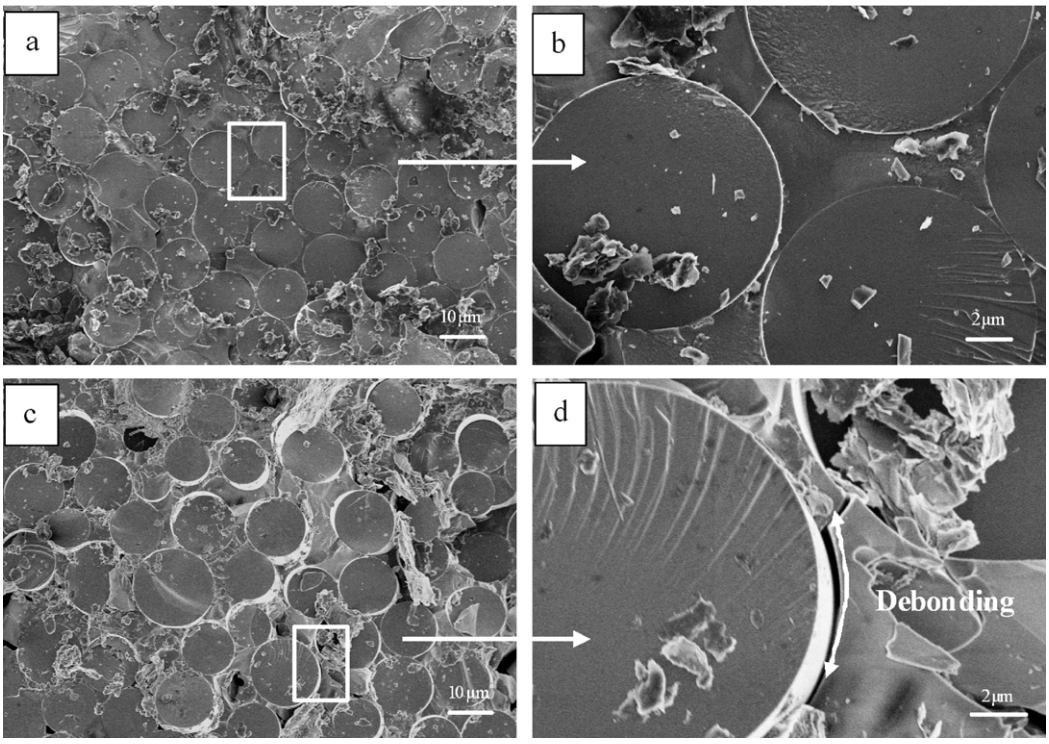

Fig. 11. The fracture surface morphology of SiCf/SiC composites without and with BN interphase.

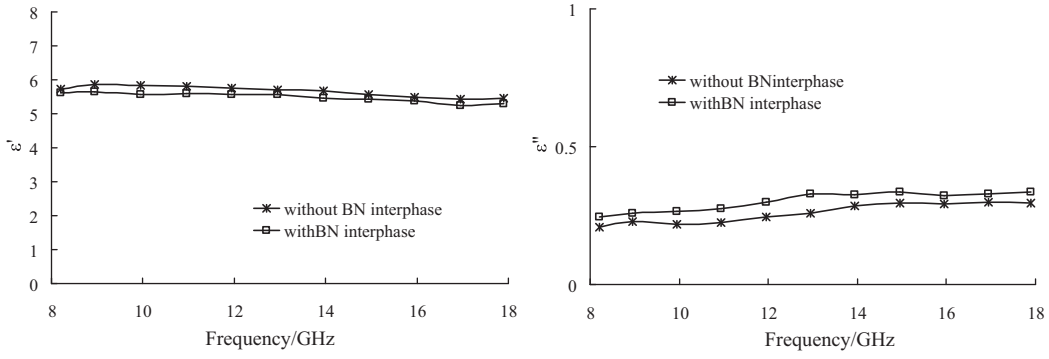

Fig. 12. The complex permittivity of SiCf/SiC composites without and with BN interphase.

reinforced mechanisms be out of service, and a brittle fracture behavior occurs.

However, for the SiCf/SiC composites with BN interphase, the BN interphase with layered crystal structure can weaken the interfacial bonding and effectively improve the accommodation between the fiber and matrix. Due to the proper combination between the fiber and matrix, most matrix cracks deflect, round when they meet the BN interphase during fracture process of the composites. As a result, the roughing effect of fiber enhances and the flexural strength of the SiCf/SiC composites is considerably improved.

3.5. Effects of BN interphase on the microwave dielectric properties of SiCf/SiC composites

The complex permittivity of SiCf/SiC composites without and with BN interphase is shown in Fig. 12. It can be found that the BN interphase has little influence on the microwave dielectric properties of SiCf/SiC composites, which is ascribed to the close dielectric properties between SiC and BN.[29]

4. Conclusions

1. t-BN is formed using boric acid and urea as precursor at 1000 °C for 1 h under N_2 atmosphere.
2. The relatively compact and continuous BN coating can be attained after three times of dipping-annealing treatment. The tensile strength of SiC fiber decreases about 30% after BN coating treatment, but the electrical resistivity of SiC fiber is nearly constant.
3. After three times of BN interphase treatment, the flexural strength of SiCf/SiC composites with BN interphase is about 2 times that of SiCf/SiC composites without BN interphase,

which is ascribed to the interfacial improvement on account of the introduction of BN interphase.

4. Due to the close dielectric properties between SiC and BN, the complex permittivity of SiCf/SiC composites without and with BN interphase is similar.

References

1. Bansal NP. *Handbook of ceramic composites*. Kluwer Academic Publisher; 2005.
2. Chawla KK. *Ceramic matrix composites*. London: Chapman and Hall; 1993.
3. Li ZM, Zhou WC, Su XL, Luo F, Huang YX, Wang C. Effect of boron doping on microwave dielectric properties of SiC powder synthesized by combustion synthesis. *J Alloys Compd* 2011;**509**(3):973–6.
4. Jin HB, Cao MS, Zhou W, Simeon A. Microwave synthesis of Al-doped SiC powders and study of their dielectric properties. *Mater Res Bull* 2010;**45**(2):247–50.
5. Luo F, Huan J, Zhu DM, Zhou WC. Dielectric properties of SiC/LAS composite. *Mater Lett* 2005;**59**(1):105–9.
6. Li XM, Zhang LT, Yin XW, Yu ZJ. Mechanical and dielectric properties of porous Si_3N_4-SiC(BN) ceramic. *J Alloys Compd* 2010;**490**(1–2):40–3.
7. Li XM, Zhang LT, Yin XW, Feng LY, Li Q. Effect of chemical vapor infiltration of SiC on the mechanical and electromagnetic properties of Si_3N_4-SiC ceramic. *Scripta Mater* 2010;**63**(6):657–60.
8. Luo F, Zhu DM, Zhou WC. A two-layer dielectric absorber covering a wide frequency range. *Ceram Int* 2007;**33**:197–200.
9. Ding DH, Zhou WC, Zhang B, Luo F, Zhu DM. Complex permittivity and microwave absorbing properties of SiC fiber woven fabrics. *J Mater Sci* 2011;**46**:2709–14.
10. Chollon G, Pailler R, Canet R, Delhaes P. Correlation between microstructure and electrical properties of SiC-based fibres derived from organosilicon precursors. *J Eur Ceram Soc* 1998;**18**:125–33.
11. Scholz R, Dos Santos Marques F, Riccardi B. Electrical conductivity of silicon carbide composites and fibers. *J Nucl Mater* 2002;**307–311**:1098–101.
12. Mouchon E, Colomban PH. Microwave absorbent: preparation, mechanical properties and r.f.-microwave conductivity of SiC (and/or mullite) fibre reinforced Nasicon matrix composites. *J Mater Sci* 1996;**31**:323–34.
13. Kassiba A, Tabellout M, Charpentier S, Herlin N, Emery JR. Conduction and dielectric behaviour of SiC nano-sized materials. *Solid State Commun* 2000;**115**:389–93.
14. Kotani M, Inoue T, Kohyama A, Okamura K, Katoh Y. Consolidation of polymer-derived SiC matrix composites: processing and microstructure. *Compos Sci Technol* 2002;**62**:2179–88.
15. Yamada R, Taguchi T, Igawa N. Mechanical and thermal properties of 2D and 3D SiC/SiC composites. *J Nucl Mater* 2000;**283–287**:574–8.
16. Sayano A, Sutoh C, Suyama S, Itoh Y, Nakagawa S. Development of a reaction-sintered silicon carbide matrix composite. *J Nucl Mater* 1999;**271–272**:467–71.
17. Naslain R. Design, preparation and properties of non-oxide CMCs for application in engines and nuclear reactors: an overview. *Comp Sci Technol* 2004;**64**:155–70.
18. Liu HT, Cheng HF, Wang J, Tang GP. Dielectric properties of the SiC fiber-reinforced SiC matrix composites with the CVD SiC interphases. *J Alloys Compd* 2010;**491**:248–51.
19. Udayakumar A, Sri Ganesh A, Raja S, Balasubramanian M. Effect of intermediate heat treatment on mechanical properties of SiC_f/SiC composites with BN interphase prepared by ICVI. *J Eur Ceram Soc* 2011;**31**:1145–53.
20. Li JS, Zhang CR, Li B. Preparation and characterization of boron nitride coatings on carbon fibers from borazine by chemical vapor deposition. *Appl Surf Sci* 2011;**257**:7752–7.
21. Wu HT, Chen MW, Wei X, Ge M, Zhang WG. Deposition of BN interphase coatings from B-trichloroborazine and its effects on the mechanical properties of SiC/SiC composites. *Appl Surf Sci* 2010;**257**:1276–81.
22. Jacques S, Lopez-Marure A, Vincent C, Vincent H, Bouix J. SiC/SiC minicomposites with structure-graded BN interphases. *J Eur Ceram Soc* 2000;**20**:1929–38.
23. Lii DF, Huang JL, Tsui LJ, Lee SM. Formation of BN films on carbon fibers by dip-coating. *Surf Coat Technol* 2002;**150**:269–76.
24. Liu HT, Cheng HF, Wang J, Che RC, Tang GP, Ma QS. Effects of the fiber surface characteristics on the interfacial microstructure and mechanical properties of the KD SiC fiber reinforced SiC matrix composites. *Mater Sci Eng A* 2009;**525**:121–7.
25. Dietrich D, Martin PW, Nestler K, Stockel S, Weise K, Marx G. Transmission electron microscopic investigations on SiC- and BN-coated carbon fibres. *J Mater Sci* 1996;**31**:5979–84.
26. Termoss H, Toury B, Brioude A, Dazord J, Brusq JL, Miele P. High purity boron nitride thin films prepared by the PDCs route. *Surf Coat Technol* 2007;**201**:7822–8.
27. Moulder JF, Stickle WF, Sobol PE, Bomben KD. *Handbook of X-ray photoelectron spectroscopy*. USA: Perkin-Elmer Corp.; 1992.
28. Toury B, Miele P, Cornu D, Vincent H, Bouix J. Boron nitride fibres prepared from symmetric and asymmetric alkylaminoborazine. *Adv Funct Mater* 2002;**12**:228–34.
29. Arya SPS, Amico AD. Preparation, properties and applications of boron nitride thin films. *Thin Solid Films* 1988;**157**:267–82.